

Figure 3. Orbital energy plot showing the variations in  $e(\pi)$  and  $a_1(\pi)$  levels as a function of distance between interacting  $\pi$  bonds.

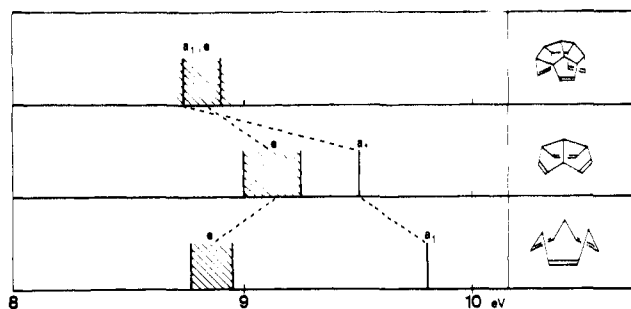


Figure 4. Correlation of the ionization energies of 1-3.

Table I. Comparison between the Ionization Potentials and Molecular Orbital Energies of  $C_{16}$ -Hexaquinacene (**1**)<sup>a</sup>

band	$I_v$	assignment	$-\epsilon_j$ (MINDO/3)
①	8.74	$a_1(\pi)$	8.94
②		$e(\pi)$	9.41
③			
④	9.9	$a_2(\sigma)$	9.75

<sup>a</sup> All values are in electron volts.

separated by 2.85 Å, the split between  $e(\pi)$  and  $a_1(\pi)$  should be below 0.5 eV. The first band is therefore assigned to ionization from  $e(\pi)$  as well as  $a_1(\pi)$  (see Table I). This assignment is supported by MO calculations of the MINDO/3 type,<sup>14</sup> assuming the validity of Koopmans' theorem.<sup>15</sup>

These calculations predict  $a_1(\pi)$  to reside above  $e(\pi)$  owing to the strong interaction of  $a_1(\pi)$  with  $a_1(\sigma)$  as in the case of **2**. In Figure 3, we have plotted the orbital energy of  $e(\pi)$  and  $a_1(\pi)$  of **1** as a function of the distance between the  $\pi$  segments. For this purpose, extended Hückel calculations were utilized.<sup>16</sup> Like the MINDO/3 method, this procedure predicts a crossing of  $a_1(\pi)$  and  $e(\pi)$  at 2.6 Å, thereby also implicating the sequence  $a_1(\pi)$ ,  $e(\pi)$  for **1**.

The ionization energies of **1-3** are correlated in Figure 4. As a result of the more extended  $\sigma$  framework in **1** relative to **2** and **3**, the center of gravity is shifted toward lower energy. As a direct consequence of the larger distance between its  $\pi$  bonds, homoconjugation in **1** is completely overridden by hyperconjugation.

The essentially ineffective  $\sigma$  overlap of the  $p\pi$  orbitals in **1** has decided chemical ramifications. Thus, the triene is totally inert to attempted reduction with potassium in liquid ammonia or oxidation with  $\text{Co}(\text{Az})_3$  in a flow-through system.<sup>17</sup>

The electronic nature of **1** would appear to rule out the likelihood that neutral homoaromatic character will ever be uncovered.

**Acknowledgments.** The authors are grateful to the donors of the Petroleum Research Fund, administered by the American Chemical Society (G.G.C.), the National Institutes of Health (Grant AI-11490, LAP), the Deutsche Forschungsgemeinschaft (R.G.), and the Fonds der Chemischen Industrie (R.G.) for financial support. Thanks are also due Mrs. H. Roth for the PE spectral measurement and Dr. Joseph Cassim for the use of his UV spectrometer.

## References and Notes

- (1) L. A. Paquette, R. A. Snow, J. L. Muthard, and T. Cynkowski, *J. Am. Chem. Soc.*, **100**, 1600 (1978). The structurally related, but conformationally disparate, *cis*-<sup>2</sup>-1,5,9-cyclododecatriene molecule has also been synthesized: K. G. Untch and D. J. Martin, *J. Am. Chem. Soc.*, **87**, 3518 (1965).
- (2) L. A. Paquette, T. G. Wallis, T. Kempe, G. G. Christoph, J. P. Springer, and J. Clardy, *J. Am. Chem. Soc.*, **99**, 6946 (1977).
- (3) (a) L. A. Paquette, *Angew. Chem.*, **90**, 114 (1978); *Angew. Chem., Int. Ed. Engl.*, **17**, 106 (1978); (b) P. M. Warner in "Topics in Nonbenzenoid Aromatic Chemistry", Vol. II, Hirokawa Publishing Co., Tokyo, 1977.
- (4) P. Bischof, R. Gleiter, and E. Heilbronner, *Helv. Chim. Acta*, **53**, 1425 (1970).
- (5) W. R. Roth, W. B. Bang, P. Göbel, R. L. Sass, R. B. Turner, and A. P. Yü, *J. Am. Chem. Soc.*, **86**, 3178 (1964).
- (6) E. D. Stevens, J. D. Kramer, and L. A. Paquette, *J. Org. Chem.*, **41**, 2266 (1976).
- (7) J. C. Bünzli, D. C. Frost, and L. Weller, *Tetrahedron Lett.*, 1159 (1973).
- (8) P. Bischof, D. Bosse, R. Gleiter, M. J. Kukla, A. de Meljere, and L. A. Paquette, *Chem. Ber.*, **108**, 1218 (1975).
- (9) (a) R. C. Kelly, Ph.D. Thesis, Harvard University, 1965; (b) L. W. Pickett, M. Muntz, and E. M. McPherson, *J. Am. Chem. Soc.*, **73**, 4862 (1951).
- (10) Internal agreement indices for the multiply measured data are
 
$$R' = \left[ \frac{\left( \sum_{hkl} \sum_{j=1}^{n_j} |F_j - F_{av}| \right)}{\left( \sum_{hkl} (n_j - 1) F_{av} \right)} \right] = 0.048$$

$$R'' = \left[ \frac{\left( \sum_{hkl} \sum_{j=1}^{n_j} w |F_j^2 - F_{av}^2| \right)}{\left( \sum_{hkl} w (n_j - 1) F_{av}^2 \right)} \right] = 0.049$$
- (11) G. G. Christoph and M. A. Beno, *J. Am. Chem. Soc.*, **100**, 3156 (1978).
- (12) The following computer programs were used: CRYM Crystallographic Computing System (D. J. DuChamp); RAGGLS, Rigid and Generalized Group Least Squares program (G. G. Christoph); REEKE Fourier program (G. N. Reeke); and ORTEP (C. R. Johnson). Atomic form factors were taken from Vol. III of the "International Tables for X-Ray Crystallography", Kynoch Press, Birmingham, England, 1962.
- (13) M. I. Davis and T. W. Muecke, *J. Phys. Chem.*, **74**, 1104 (1970).
- (14) R. C. Bingham, M. J. S. Dewar, and D. H. Lo, *J. Am. Chem. Soc.*, **97**, 1285 (1975). The program actually used was that described by P. Bischof, *J. Am. Chem. Soc.*, **98**, 6844 (1976).
- (15) T. Koopmans, *Physica (Utrecht)*, **1**, 104 (1934).
- (16) R. Hoffmann, *J. Chem. Phys.*, **39**, 1397 (1972); R. Hoffmann and W. N. Lipscomb, *ibid.*, **38**, 2179, 3489 (1962); **37**, 2872 (1962).
- (17) H. Bock, private communication.
- (18) The Ohio State University Dissertation Fellow, 1977-1978.

Gary G. Christoph,\* Jean L. Muthard,<sup>18</sup> Leo A. Paquette\*

Evans Chemical Laboratories  
The Ohio State University  
Columbus, Ohio 43210

Michael C. Böhm, Rolf Gleiter\*

Institut für Organische Chemie  
Technische Hochschule Darmstadt  
D6100 Darmstadt, West Germany

Received June 27, 1978

## Static and Dynamic Stereochemistry of Dicoordinate Phosphorus Cations

Sir:

It has been demonstrated<sup>1,2</sup> that halide ion abstraction from halophosphines results in apparently dicoordinate phosphorus

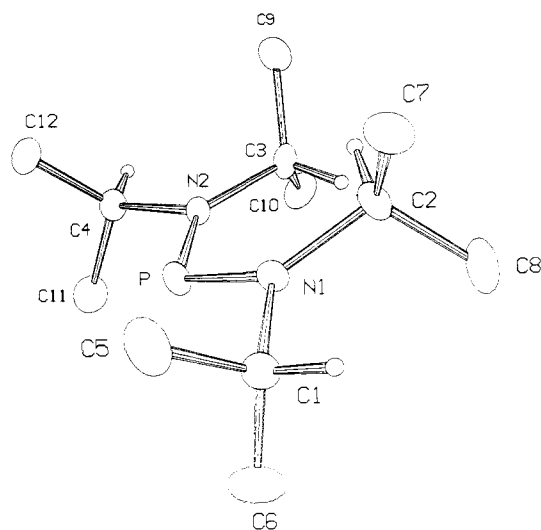


**Figure 1.** ORTEP drawing of  $[(i\text{-Pr}_2\text{N})_2\text{P}]^+$  (**2**). The thermal ellipsoids are drawn at the 20% probability level. The Me hydrogens are omitted.

cations such as  $[(\text{Me}_2\text{N})_2\text{P}]^+$  (**1**),  $[\text{Me}_2\text{NPCl}]^+$ , and  $[\text{MeNCH}_2\text{CH}_2\text{N}(\text{Me})\text{P}]^+$ . These cations have attracted considerable attention because, possessing both a lone pair of electrons and a formally vacant orbital on phosphorus, they can function as either Lewis acids<sup>3</sup> or act as ligands toward metal carbonyls.<sup>4,5</sup> Here we report the first X-ray crystal structure data for this class of compound. These data confirm the structure suggested for **1** on the basis of NMR evidence by Parry and co-workers.<sup>2</sup> Some new NMR data pertinent to the dynamic stereochemistry of dicoordinate phosphorus cations are also presented.

White, crystalline  $[(i\text{-Pr}_2\text{N})_2\text{P}]^+[\text{AlCl}_4]^-$  (**2**) was prepared by treating  $(i\text{-Pr}_2\text{N})_2\text{PCl}^6$  with an equimolar quantity of  $\text{AlCl}_3$  in  $\text{CH}_2\text{Cl}_2$  or  $\text{SO}_2^7$  solution. Crystals of **2** suitable for X-ray diffraction were grown from  $\text{CH}_2\text{Cl}_2$ -cyclohexane solution. X-ray data were collected on a Syntex P2<sub>1</sub> automated diffractometer. The crystal was maintained at  $-30^\circ\text{C}$  in a stream of dry nitrogen throughout the data collection. Compound **2** crystallizes in the tetragonal system, space group  $I4_1cd$ , with 16 molecules per unit cell of dimensions  $a = b = 19.947$  (7) and  $c = 21.363$  (4) Å. The structure was solved by direct methods.<sup>8</sup> Full-matrix least-squares refinement utilizing 1747 observed reflections yielded a conventional  $R$  value of 0.044.

The conformation of the phosphorus cation, **2**, is depicted in Figure 1, and a summary of pertinent bond distances and angles appears in Table I. The geometry at the cationic center can be understood in terms of approximate trigonal-planar hybridization at phosphorus, diminution of the  $\text{N}(1)\text{-P-N}(2)$  bond angle from  $120$  to  $114.8^\circ$  being caused by lone pair-bond pair repulsions. Within experimental error the sum of the bond angles around each of the nitrogen atoms is  $360^\circ$ , thus indicating planar nitrogen geometries for both  $i\text{-Pr}_2\text{N}$  groups. Such an arrangement is expected on the basis of optimization of the conjugation between the nitrogen lone pairs and the formally vacant  $3p$  orbital at phosphorus. The approximately planar conformation of the subunit  $\text{C}(1)\text{C}(2)\text{N}(1)\text{PN}(2)\text{C}(3)\text{C}(4)$  is understandable on the same basis. The  $\text{N-P}$  bond distance of  $1.613$  Å in **2** is slightly shorter than those found in neutral aminophosphines.<sup>9</sup> This bond shortening is presumably due to a combination of the formal positive charge at phosphorus and the  $\text{N} \rightarrow \text{P}$  dative  $\pi$  bonding discussed above.

There are some indications of the operation of steric effects in **2**. For example, the cation does not quite possess a plane of symmetry since, in fact, the dihedral angle between the two  $>\text{N-P}$  planes is  $\sim 18^\circ$ . Relief of steric strain may also be responsible for the fact that, within each  $>\text{N-P}$  plane, one of the angles about nitrogen is significantly larger than the other

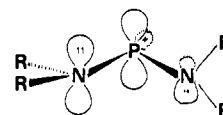


**Figure 2.** Computed<sup>11</sup> transition state for  $\text{N-P}$  rotation in  $[(\text{R}_2\text{N})_2\text{P}]^+$  cations.

**Table I.** Bond Lengths (Ångstroms) and Angles (Degrees) for the Dicoordinate Phosphorus Cation,  $[(i\text{-Pr}_2\text{N})_2\text{P}]^+$

bond lengths		bond angles	
P-N(1)	1.611 (0.004)	N(1)-P-N(2)	114.8 (0.2)
P-N(2)	1.615 (0.004)	P-N(1)-C(1)	112.3 (0.3)
N(1)-C(1)	1.530 (0.006)	P-N(1)-C(2)	132.9 (0.3)
N(1)-C(2)	1.500 (0.006)	C(1)-N(1)-C(2)	114.7 (0.3)
N(2)-C(3)	1.497 (0.006)	P-N(2)-C(3)	132.1 (0.3)
N(2)-C(4)	1.526 (0.005)	P-N(2)-C(4)	112.5 (0.3)
		C(3)-N(2)-C(4)	115.4 (0.3)

two.<sup>10</sup> It is interesting to note, however, that molecular orbital (MO) calculations<sup>11</sup> (with geometry optimization) indicate that comparable distortions exist in cations with less bulky substituents such as **1** and  $[(\text{NH}_2)_2\text{P}]^+$ .

Previous DNMR spectroscopic work<sup>2</sup> on **1** showed temperature independent  $^1\text{H}$  spectra below  $-35^\circ\text{C}$ , revealing two distinct Me environments. Similar spectral behavior is observed for **2** in that two Me resonances, resulting from nonequivalent isopropyl groups, reach minimum line width at  $-75^\circ\text{C}$ . These observations are compatible with the ground-state geometry determined for **2** by X-ray crystallography. The fact that the barrier for the stereochemical interchange of Me groups is less for **2** (11.1 kcal/mol) than **1** (14.6 kcal/mol) is most logically ascribed to steric destabilization of the ground state. Equivalencing of the Me environments in **1** and **2** could occur via  $\text{N-P}$  bond rotation and/or inversion at the  $\text{P}^+$  center becoming rapid on the NMR time scale. To probe this question we have prepared the "mixed" cation,  $[(i\text{-Pr}_2\text{N})(\text{Me}_2\text{N})\text{P}]^+$  (**3**), and examined its fluxional behavior by  $^1\text{H}$  DNMR spectroscopy. Interestingly, we find that **3** exhibits *two* coalescence phenomena, the barriers pertaining to the  $i\text{-Pr}_2\text{N}$  and  $\text{Me}_2\text{N}$  moieties being 11.5 and 12.6 kcal/mol, respectively. This observation indicates that equivalencing of the isopropyl groups in **3** occurs via  $\text{N-P}$  bond rotation because inversion at  $\text{P}^+$  would require both dialkylamino groups to undergo coalescence simultaneously. Since the barrier magnitude in **3** for the  $i\text{-Pr}_2\text{N}$  group is very similar to that in the symmetrically substituted cation, **2**, it may be presumed that the dynamic behavior of **2** is also due to rotation around the  $\text{N-P}$  bonds. This conclusion agrees with MNDO calculations<sup>11</sup> on **1** and ab initio calculations<sup>11</sup> on  $[(\text{NH}_2)_2\text{P}]^+$  which indicate that the barrier to phosphorus inversion is significantly larger than that due to  $\text{N-P}$  rotation. The MO calculations indicate further that the geometry of the rotational transition state is that indicated in Figure 2. Thus, as rotation proceeds around a given  $\text{N-P}$  bond, the rest of the cation remains fixed in order to minimize the loss of  $p\pi\text{-}p\pi$  conjugation.

**Acknowledgments.** The authors are grateful to the National Science Foundation (Grant CHE 76-10331) and the Robert A. Welch Foundation for generous financial support. The X-ray equipment was purchased through a grant (GP-37028) from the National Science Foundation.

## References and Notes

- S. Fleming, M. K. Lupton, and K. Jekot, *Inorg. Chem.*, **11**, 2534 (1972).
- M. G. Thomas, C. W. Schultz, and R. W. Parry, *Inorg. Chem.*, **16**, 994 (1977).
- C. W. Schultz and R. W. Parry, *Inorg. Chem.*, **15**, 3046 (1976).
- R. W. Light and R. T. Paine, *J. Am. Chem. Soc.*, **100**, 2230 (1978).

- (5) R. G. Montemayer, D. T. Sauer, S. Fleming, D. W. Bennett, M. G. Thomas, and R. W. Parry, *J. Am. Chem. Soc.*, **100**, 2231 (1978).
- (6) The synthesis and characterization of  $(i\text{-Pr}_2\text{N})_2\text{PCl}$ ,  $(i\text{-Pr}_2\text{N})(\text{Me}_2\text{N})\text{PCl}$ , and other N-P compounds will be described in a subsequent publication.
- (7) In separate experiments we have established that  $(i\text{-Pr}_2\text{N})_2\text{PCl}$  reacts with  $\text{SO}_2$  in the absence of  $\text{AlCl}_3$  at ambient temperature to afford  $(i\text{-Pr}_2\text{N})_2\text{-P}(\text{O})\text{Cl}$ .
- (8) Program MULTAN: M. M. Woolfson, J. P. Declercq, and G. Germain.
- (9) For a compilation of N-P bond distances, see, e.g., J. C. Clardy, R. L. Kolpa, and J. G. Verkade, *Phosphorus*, **4**, 133 (1974).
- (10)  $\angle\text{P-N(1)-C(2)} = 132.9(3)^\circ$ ;  $\angle\text{P-N(2)-C(3)} = 132.1(3)^\circ$ .
- (11) A. H. Cowley and M. McKee, unpublished work.

Alan H. Cowley,\* Mike C. Cushner, John S. Szobota

Department of Chemistry  
The University of Texas at Austin  
Austin, Texas 78712

Received August 28, 1978

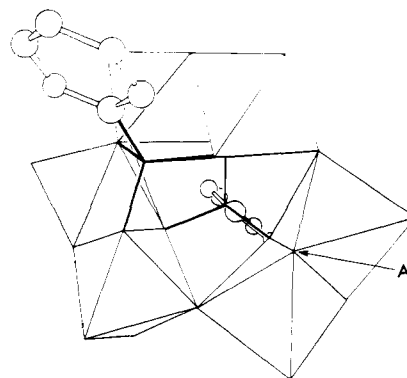


Figure 1. The structure of  $[(\text{PhAs})_2\text{W}_6\text{O}_{25}\text{H}]^{5-}$  and  $[(\text{PhAs})_2\text{Mo}_6\text{O}_{25}\text{H}_2]^{4-}$  as a ring of six  $\text{MO}_6$  octahedra linked by shared edges (three), corners (two), and faces (one) and capped on either side by  $\text{PhAsO}_3$  groups. The vertex labeled A represents  $\text{OH}^-$  in the tungstate and  $\text{H}_2\text{O}$  in the molybdate.

### Protonation-Induced Dynamic Stereochemistry of Hexatungstobis(organoarsonate) Anions

Sir:

The formation of heteropoly and isopoly complexes from monomeric oxo anions must involve sequences of protonation and water elimination steps which have so far eluded direct observation. We report here a heteropoly tungstate structure, protonation of which leads to fluxional behavior involving exchange of coordinated water.

Aqueous solutions of tungstate and organoarsenate anions,  $\text{RAsO}_3^{2-}$ , react at pH 5-7 to form the heteropoly anions  $(\text{RAs})_2\text{W}_6\text{O}_{25}\text{H}^{5-}$ , which can be isolated as guanidinium salts.<sup>1</sup> The salt  $(\text{CN}_3\text{H}_6)_5[(\text{C}_6\text{H}_5\text{As})_2\text{W}_6\text{O}_{25}\text{H}]\cdot 2\text{H}_2\text{O}$ , crystallizes as well-formed parallelepipeds in space group  $Pbca$  with  $a = 22.050(5)$ ,  $b = 21.614(4)$ ,  $c = 19.680(4)$  Å;  $Z = 8$ ;  $\rho(\text{calcd}) = 3.04$ ,  $\rho(\text{obsd}) = 3.04(1)$  g  $\text{cm}^{-3}$ . Its crystal structure was determined by direct methods from 4238 independent nonzero diffraction intensities measured with a Picker FACS-I diffractometer using Zr-filtered Mo  $K\alpha$  radiation. The structure was refined by full-matrix least squares to final consistency indices of  $R = 0.065$  and  $R_w = 0.077$ . Complete crystallographic and structural details will appear later, but the important features of the anion are shown in Figure 1. The anion is isostructural with  $[(\text{C}_6\text{H}_5\text{As})_2\text{Mo}_6\text{O}_{25}\text{H}_2]^{4-}$ ,<sup>2,3</sup> and is the first example of a structure involving face-shared  $\text{WO}_6$  octahedra. We have argued previously, on the basis of metal-oxygen bond lengths, that the two nonaromatic protons in the molybdate structure formed a bridging water molecule at one of the vertices of the shared octahedral face (see Figure 1). Analogous arguments place the single proton (required by the cation stoichiometry) on the corresponding vertex of the tungstate structure. The W-O(H) bond lengths are 2.14(2) and 2.16(2) Å compared with 2.39(2) and 2.48(2) Å for Mo-O(H<sub>2</sub>).<sup>4</sup>

Although the two organic groups on either side of the anion are not structurally equivalent, only a single  $^1\text{H}$  NMR signal is seen for solutions of the molybdates in water or "wet" organic solvents.<sup>2</sup> It was suggested that equalization of the organic groups resulted from rapid exchange of the anion's bridging water molecule with the solvent. Such an exchange was postulated to involve an "anhydrous" intermediate of  $D_{3d}$  symmetry in which all six  $\text{MoO}_6$  octahedra are linked by shared edges.<sup>5</sup> In contrast to the molybdates, NMR spectra of the new tungstate complexes show two signals which coalesce as the pH is lowered. Spectra of the phenyl derivative are shown in Figure 2. Above pH 3.6 the ortho proton resonances appear as a pair of multiplets at ~8.1 and 8.4 ppm, whereas the meta and para protons of both phenyl groups form an unresolved multiplet in the same region (~7.7 ppm) as the five protons of uncomplexed phenylarsonate. When the pH is lowered the

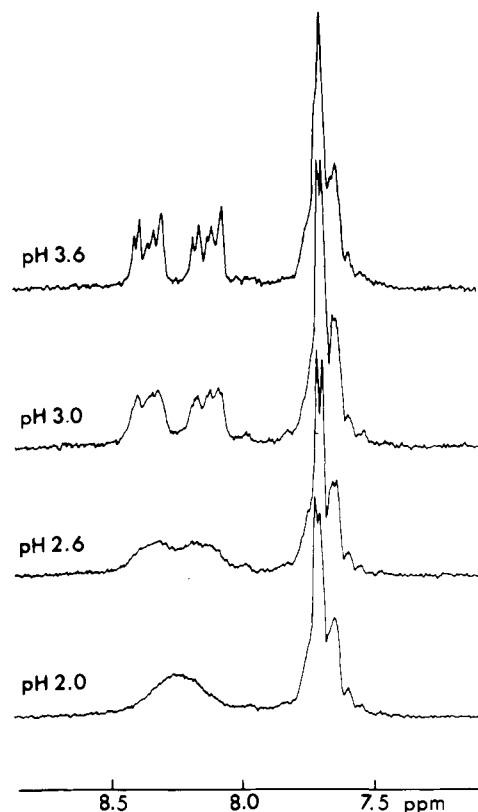


Figure 2. 90-MHz  $^1\text{H}$  FT-NMR spectra of 0.017 M  $(\text{C}_6\text{H}_5\text{As})_2\text{W}_6\text{O}_{25}\text{H}^{5-}$  prepared by mixing stoichiometric quantities of  $\text{D}_2\text{O}$  solutions of  $\text{Na}_2\text{WO}_4$  and  $\text{C}_6\text{H}_5\text{AsO}_3\text{H}_2$  and adjusting the pH with  $\text{DCl}$  (temperature,  $26^\circ\text{C}$ ). The spectrum of an analyzed sample of the sparingly soluble guanidinium salt of pH 7 was identical with the top spectrum shown.

ortho resonances broaden and coalesce, but the ratio of intensities, ortho:(meta + para), remains unchanged, showing that there has been no net decomposition of the complex. The spectra support a process that involves protonation of the bridging hydroxo oxygen and subsequent water exchange as for the molybdate. Preliminary line-shape analysis of the NMR spectrum of  $(\text{CH}_3\text{As})_2\text{W}_6\text{O}_{25}\text{H}^{5-}$  at pH 4.2 and  $26\text{-}90^\circ\text{C}$  gave apparent activation parameters,  $\Delta H^\ddagger \sim 12$  kJ  $\text{mol}^{-1}$  and  $\Delta S^\ddagger \sim -170$  J  $\text{K}^{-1}$   $\text{mol}^{-1}$ . Such parameters are not inconsistent with a mechanism involving a protonation pre-equilibrium followed by water exchange, although further investigation of this system is required and is planned. The difference in lability between the molybdate and tungstate anions may only reflect differences in basicity. Since exchange-averaged NMR spectra were observed for the molybdates over the complete pH range of stability, the  $pK$  for